J Mater Sci (2008) 43:5851–5860
DOI 10.1007/s10853-008-2841-5

Stiffness and energy dissipation in polyurethane auxetic foams

Matteo Bianchi · Fabrizio L. Scarpa · Christopher W. Smith

Received: 21 April 2008 / Accepted: 25 June 2008 / Published online: 28 July 2008

Abstract Auxetic open cell polyurethane (PU) foams have been manufactured and mechanically characterised under cyclic tensile loading. The classical manufacturing process for auxetic PU foams involves multiaxial compression of the conventional parent foam, and heating of the compressed specimens above the T_m of the foam polymer. Eighty cylindrical specimens were fabricated using manufacturing routes modified from those in the open literature, with different temperatures (135 °C, 150 °C), compression ratios and different cooling methods (water or room temperature exposure). Compressive tensile cyclic loading has been applied to measure tangent modulus, Poisson's ratios and energy dissipated per unit volume. The results are used to obtain relations between manufacturing parameters, mechanical and hysteresis properties of the foams. Compression, both radial and axial, was found to be the most significant manufacturing parameter for the auxetic foams in this work.

Introduction

The seminal work of Lakes in 1987 [1] opened the field of modelling, manufacturing and testing of auxetic materials and structures for engineering applications. The negative Poisson's ratio effect is allowed in classical elasticity for isotropic, homogeneous and thermodynamically correct solids, ranging between −1 and 0.5 for 3D unconstrained media [2], while for special orthotropic materials the only limits for the Poisson's ratios are given by the equivalence between cross products of Young's moduli and Poisson's ratios in the same plane [3]. The negative Poisson's ratio effect, therefore, reveals itself as a counter-intuitive deformation behaviour, with unusual large volume changes. Negative Poisson's ratio has been observed also in balanced symmetric cross-ply laminates [4–6], microporous polyethylene [7, 8], centresymmetric [9–11] and non-centresymmetric cellular configurations [12, 13]. Lakes [1] produced an open cell foam with a Poisson's ratio −0.7 using industrial thermoplastic Scott foam. Subsequently, several polymeric and metal foams were transformed into auxetic phase [14], showing enhancement in terms of indentability [15] and viscoelastic loss [16, 17] compared to the conventional base used for their fabrication. The increase in terms of sound absorption coefficients was recorded for the first time by Howell et al. [18], and confirmed for high-density auxetic open cell foams by Scarpa et al. [19]. Chan and Evans [20] outlined a manufacturing route for auxetic open cell thermoplastic foams, which was then followed by Gaspar et al. [21], and modified by Scarpa et al. [22], to obtain NPR specimens with high resilience [23], improved stiffness [22], and high energy dissipation per unit volume under compressive cyclic fatigue loading [24].

In the above-cited works, only a limited number of auxetic specimens have been produced and tested in part because of the mechanical and thermal energies involved in the classic manufacturing process, as well as the discard rate and difficulty of obtaining clean specimens. Although an initial attempt has been made in [22], it is in general difficult to identify relations between the manufacturing

M. Bianchi · F. L. Scarpa
Department of Aerospace Engineering, University of Bristol, Queens Building, BS8 1TR Bristol, UK

C. W. Smith (✉)
School of Engineering, Computing and Mathematics, University of Exeter, North Park Road, EX4 4QF Exeter, UK
e-mail: c.w.smith@ex.ac.uk

parameters and the final mechanical properties of the foam with a limited statistical population of specimens. In this work, eighty specimens were manufactured in 16 batches following a modification of the manufacturing process [22] with two cooling systems that have been mechanically tested, measuring the stiffness, Poisson's ratio and hysteresis at 0.03 Hz tensile cyclic loading. General relationships between the initial volumetric ratio (IVR) and final density ratios (FDR), and the mechanical properties have been clearly identified for the Poisson's ratio (v) and the tangent modulus, while the loss tangent (tan δ) assumes a more scattered behaviour with no clear correlation with the manufacturing parameters.

Materials and equipment

The specimens tested were obtained from conventional grey open-cell polyurethane (PU) foams supplied by McMaster-Carr Co, Chicago, IL, with 1181–1378 pores/m, and 27.2 kg/m^3 density. The native foam was provided in square blocks of 600 mm side length and 50 mm thickness. Cylindrical specimens of foam were then cut using a sharp edged tube so that the rise direction of the foam lay in the long axis of the sample. The various manufacturing parameters thought to control final mechanical properties were varied in a systematic manner. Two types of tubes (30 and 48 mm in diameter) were employed to provide different compression ratios. Sixteen batches (five specimens each) were manufactured, each batch being characterised by the maximal temperature, radial compression, heating duration and cooling method. Within each batch, specimens were subjected to different axial compressions, ranging from 1.25 to 5. In all, 80 different specimens were manufactured with volumetric compression ratios ranging from 5 to 19.1, see Table 1.

The conversion process applied to the foams involved the imposition of a two axis compression, followed by heating until softening, with an ensuing cooling process (still under mechanical compression), which was carried out in one of two different ways. The aluminium mould used consisted of a set of five tubes and piston rods able to slide along the tubes independently. Different values of axial compression could be achieved by altering the position of the piston in the tubes. The internal wall of the tube was lubricated with olive oil because distilled oils or oil-derivatives show instability and unpleasant smells at high temperatures [15, 22]. The foam specimens were carefully inserted inside the tubes using a wire to even out the deformation in the foam avoiding as far as possible the formation of creases or torque effects. A conical inlet proved useful in avoiding creases, especially for the specimens with larger initial diameters. The mould was then put into an industrial convection oven (Sanyo MOV-212F).

A number of preliminary batches were made in order to optimise the time–temperature profile. During the preliminary tests, many specimens were auxetic for only a few hours following manufacture, while others exhibited conventional positive Poisson's ratios. The eventual optimised method involved is preheating the oven to 200 °C and then putting the mould into the oven to heat. To monitor specimen temperature, a thermocouple was inserted between the mould and the foam specimen. Two time–temperature profiles (135 °C in 12 min and 150 °C in 15 min) were applied to both sets of specimens, one with 48 mm and the other with 30 mm diameter, as shown in Fig. 1.

The heating process was followed by a cooling operation. Two methods of cooling were tested: firstly, cooling in air at room temperature lasting approximately one and half hours; secondly, cooling in room water temperature lasting approximately 5 min. Following cooling, specimens were gently manipulated by hand in order to relax the external surface. All specimens' manufacturing parameters are shown in Table 1.

Experimental methods and testing techniques

Dimensions and weights of all specimens were measured to calculate their density before and after processing. Analysis including mechanical testing had to be made reasonably rapidly following processing, since they relax back to their original shape over periods of months; however for the water-cooled specimens it was necessary to wait for approximately 2 days until the core of these specimens was completely dry. For the sake of comparability between the results, dimensions and mass were measured 1 week following post-processing. Some of the batches have an unusual density value in comparison to other specimen batches due to the different cooling methods. Dimensions were measured with callipers, and mass was measured using a Mettler PM2500 electronic balance with a sensitivity of 0.001 g. All measurements were carried out in a room with a stable temperature and humidity (21 °C and 48% RH). The diameter was measured in three different positions and the mean result used. By knowing the density of the conventional foam, ρ_{conv} (27.2 kg/m^3), and the final density, ρ, of the auxetic specimens, it has been possible to calculate the FDR:

$$\text{FDR} = \frac{\rho}{\rho_{\text{conv}}} \tag{1}$$

In order to measure Poisson's ratio, tangent modulus (analogous to Young's modulus) and the dissipation of energy of each specimen, a Shimadzu Autograph AGS-

Table 1 Processing parameters for all specimens

Batch	Specimen	Initial size (mm)		Imposed size (mm)		Compression ratio			Temperature (°C)	Time (min)	Cooling method
		Diameter	Length	Diameter	Length	Radial	Axial	Volume			
A	1A	48	180	19	60	2.53	3	19.15	135	12	Water
	2A	48	160	19	60	2.53	2.67	17.02			
	3A	48	140	19	60	2.53	2.33	14.89			
	4A	48	120	19	60	2.53	2.00	12.76			
	5A	48	100	19	60	2.53	1.67	10.64			
B	1B	48	180	19	60	2.53	3	19.15	150	15	Water
	2B	48	160	19	60	2.53	2.67	17.02			
	3B	48	140	19	60	2.53	2.33	14.89			
	4B	48	120	19	60	2.53	2.00	12.76			
	5B	48	100	19	60	2.53	1.67	10.64			
C	1C	48	180	19	80	2.53	2.25	14.36	135	12	Water
	2C	48	160	19	80	2.53	2.00	12.76			
	3C	48	140	19	80	2.53	1.75	11.17			
	4C	48	120	19	80	2.53	1.50	9.57			
	5C	48	100	19	80	2.53	1.25	7.98			
D	1D	48	180	19	80	2.53	2.25	14.36	150	15	Water
	2D	48	160	19	80	2.53	2.00	12.76			
	3D	48	140	19	80	2.53	1.75	11.17			
	4D	48	120	19	80	2.53	1.50	9.57			
	5D	48	100	19	80	2.53	1.25	7.98			
E	1E	48	180	19	80	2.53	2.25	14.36	135	12	Room temperature
	2E	48	160	19	80	2.53	2.00	12.76			
	3E	48	140	19	80	2.53	1.75	11.17			
	4E	48	120	19	80	2.53	1.50	9.57			
	5E	48	100	19	80	2.53	1.25	7.98			
F	1F	48	180	19	80	2.53	2.25	14.36	150	15	Room temperature
	2F	48	160	19	80	2.53	2.00	12.76			
	3F	48	140	19	80	2.53	1.75	11.17			
	4F	48	120	19	80	2.53	1.50	9.57			
	5F	48	100	19	80	2.53	1.25	7.98			
G	1G	30	200	19	60	1.58	3.33	8.31	135	12	Water
	2G	30	180	19	60	1.58	3.00	7.48			
	3G	30	160	19	60	1.58	2.67	6.65			
	4G	30	140	19	60	1.58	2.33	5.82			
	5G	30	120	19	60	1.58	2.00	4.99			
H	1H	30	200	19	40	1.58	5.00	12.47	135	12	Water
	2H	30	180	19	40	1.58	4.50	11.22			
	3H	30	160	19	40	1.58	4.00	9.97			
	4H	30	140	19	40	1.58	3.50	8.73			
	5H	30	120	19	40	1.58	3.00	7.48			
I	1I	30	200	19	60	1.58	3.33	8.31	150	15	Water
	2I	30	180	19	60	1.58	3.00	7.48			
	3I	30	160	19	60	1.58	2.67	6.65			
	4I	30	140	19	60	1.58	2.33	5.82			
	5I	30	120	19	60	1.58	2.00	4.99			

Table 1 continued

Batch	Specimen	Initial size (mm)		Imposed size (mm)		Compression ratio			Temperature (°C)	Time (min)	Cooling method
		Diameter	Length	Diameter	Length	Radial	Axial	Volume			
L	1L	30	200	19	40	1.58	5.00	12.47	150	15	Water
	2L	30	180	19	40	1.58	4.50	11.22			
	3L	30	160	19	40	1.58	4.00	9.97			
	4L	30	140	19	40	1.58	3.50	8.73			
	5L	30	120	19	40	1.58	3.00	7.48			
M	1M	30	200	19	40	1.58	5.00	12.47	135	12	Room temperature
	2M	30	180	19	40	1.58	4.50	11.22			
	3M	30	160	19	40	1.58	4.00	9.97			
	4M	30	140	19	40	1.58	3.50	8.73			
	5M	30	120	19	40	1.58	3.00	7.48			
N	1N	30	200	19	60	1.58	3.33	8.31	135	12	Room temperature
	2N	30	180	19	60	1.58	3.00	7.48			
	3N	30	160	19	60	1.58	2.67	6.65			
	4N	30	140	19	60	1.58	2.33	5.82			
	5N	30	120	19	60	1.58	2.00	4.99			
O	1O	30	200	19	40	1.58	5.00	12.47	150	15	Room temperature
	2O	30	180	19	40	1.58	4.50	11.22			
	3O	30	160	19	40	1.58	4.00	9.97			
	4O	30	140	19	40	1.58	3.50	8.73			
	5O	30	120	19	40	1.58	3.00	7.48			
P	1P	30	200	19	60	1.58	3.33	8.31	150	15	Room temperature
	2P	30	180	19	60	1.58	3.00	7.48			
	3P	30	160	19	60	1.58	2.67	6.65			
	4P	30	140	19	60	1.58	2.33	5.82			
	5P	30	120	19	60	1.58	2.00	4.99			
Q	1Q	48	180	19	60	2.53	3.00	19.15	135	12	Room temperature
	2Q	48	160	19	60	2.53	2.67	17.02			
	3Q	48	140	19	60	2.53	2.33	14.89			
	4Q	48	120	19	60	2.53	2.00	12.76			
	5Q	48	100	19	60	2.53	1.67	10.64			
R	1R	48	180	19	60	2.53	3.00	19.15	150	15	Room temperature
	2R	48	160	19	60	2.53	2.67	17.02			
	3R	48	140	19	60	2.53	2.33	14.89			
	4R	48	120	19	60	2.53	2.00	12.76			
	5R	48	100	19	60	2.53	1.67	10.64			

Note that within each batch there were five specimens, each with a different axial compression ratio ranging from 1.25 to 5

10kND testing machine equipped with a 50 N load cell was used. Tests were in tension and were quasi-static and cyclical (displacement rate of 20 mm/min). Deformations, and thus strains, were measured via an optical system Videoextensometer (Messphysik GmbH, Austria), which is an edge following system and required small contrasting surface markers to be adhered temporarily to specimens using a 'poster mount' type adhesive ('Spray Mount', 3M Inc). The markers were thus adhered away from the clamped ends and to only the central portion of cylindrical specimen, allowing deformation and strain data to be collected from only this central portion and avoiding ends effects [26]. Figure 2 shows how these markers remained adhered to the central portion of the foam; consequently the resulting data reflects deformations and strains down the central portion of the sample. There was nothing to suggest there was anything but uniform strain down the length of the main body of the samples.

The longitudinal and transverse strains were calculated as:

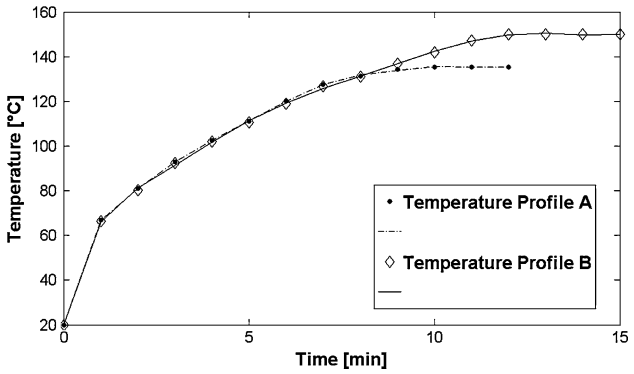

Fig. 1 Time–temperature profiles with the final value of 135 °C and 150 °C

Fig. 2 Example of a specimen with the markers ready to be tested

$$\varepsilon_x = \frac{\Delta l}{l_0}; \quad \varepsilon_y = \frac{\Delta d}{d_0} \tag{2}$$

where Δl and Δd are the longitudinal and diameter deformations, and l_0 and d_0 the starting specimen length and diameters, respectively. The Poisson's ratio v_{xy} was calculated using the classical definition for the strain data during the loading portion of the stress–strain cycle:

$$v_{xy} = -\frac{\varepsilon_y}{\varepsilon_x} \tag{3}$$

The tensile stress using the starting specimen cross section A_0 was calculated as:

$$\sigma = \frac{F}{A_0} \tag{4}$$

while the tangent modulus was calculated using the definition [7] for data during the loading portion of the stress–strain cycle:

$$E = \frac{\mathrm{d}\sigma}{\mathrm{d}\varepsilon_x} \tag{5}$$

In this case, the slope of the linear region of the stress–strain curve ranges between 0 and 5–10% strain. Most conventional foams presented a quasi-linear response during deformation before reaching 20% strain. A quasi-static tensile progressive stress–strain analysis on auxetic samples revealed that the negative Poisson's ratio foams behave linearly up to 25% of tensile strain. By considering the foam as a viscoelastic linear material, the Young's complex modulus can be represented as [25]:

$$E^* = E(1 + \mathrm{i}\tan\delta) \tag{6}$$

where δ is the phase angle between the stress and strain sinusoids. For each specimen, a stress–strain curve was measured corresponding to the cyclic loading with $R = 0$, i.e. the ratio between the minimum and maximum displacement during testing [24] ($R = 0$ indicating that the test was done in tension–tension); a typical example is

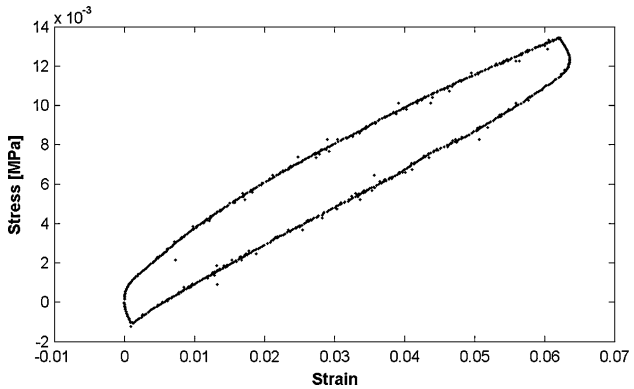

Fig. 3 Example of stress–strain curve

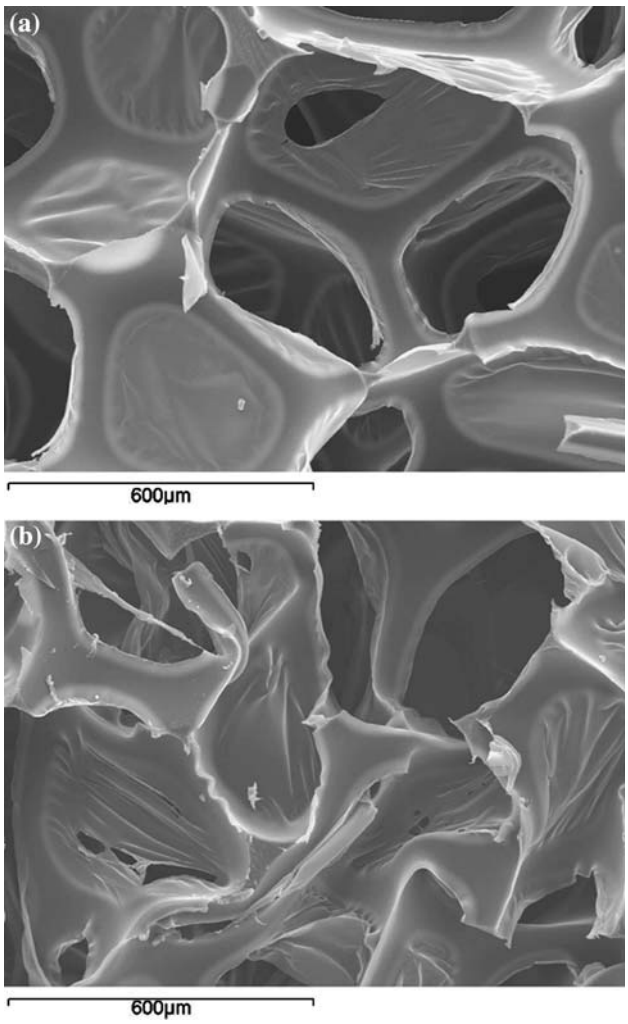

Fig. 4 SEM images of (**a**) conventional and (**b**) auxetic open cell foam

shown in Fig. 3 for specimen 1A. The areas corresponding to the hysteresis cycles were calculated by approximating the sides of each stress–strain curve with two second degree polynomial curves and subsequent numerical integration of areas.

Results and discussion

Figure 4a and b shows SEM images of the conventional and negative Poisson's ratio microstructures, respectively. The conventional parent phase foam is partially reticulated, with membranes present between the cell ribs, and average diameter around 500 μm. The negative Poisson's ratio foam (Poisson's ratio –0.24) instead shows convoluted and disordered unit cells, with complex rib geometry. Using the final density data acquired regarding each specimen and knowing the density of the native foam, an analysis of the FDR versus the imposed volumetric ratio (IVR) was carried out using a linear least squares (LLS) technique, as shown in Fig. 5. It is noticeable that all the batches show a quasi-linear trend, with the curve slopes ranging between 0.12 and 0.56. All the batches yield a good correlation factor for the LLS of approximately 0.9. A significant discrepancy between the IVR and FDR is clear. This may be so because while the IVR is a geometrical ratio, the FDR is a ratio between densities; hence any loss of mass associated with heating during processing may alter the FDR and, more importantly, become a factor in the mechanical behaviour of the auxetic specimens.

The values of force, length and width were post-processed and, in general, exhibited repeatable and linear behaviour in terms of longitudinal and lateral strains and stress. A single cycle, usually the last of five, was chosen for analysis.

All specimens were auxetic, i.e. exhibited negative Poisson's ratios, and in general specimens with lower axial compressive ratios tend to reach maximal negative Poisson's ratios, see Fig. 6. Lower Poisson's ratios were

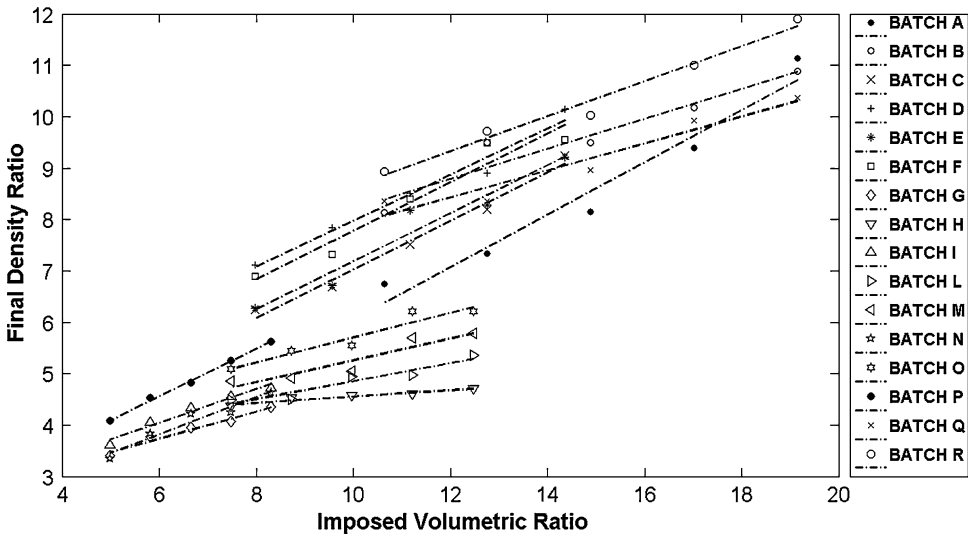

Fig. 5 Imposed volumetric ratio versus final density ratio curve

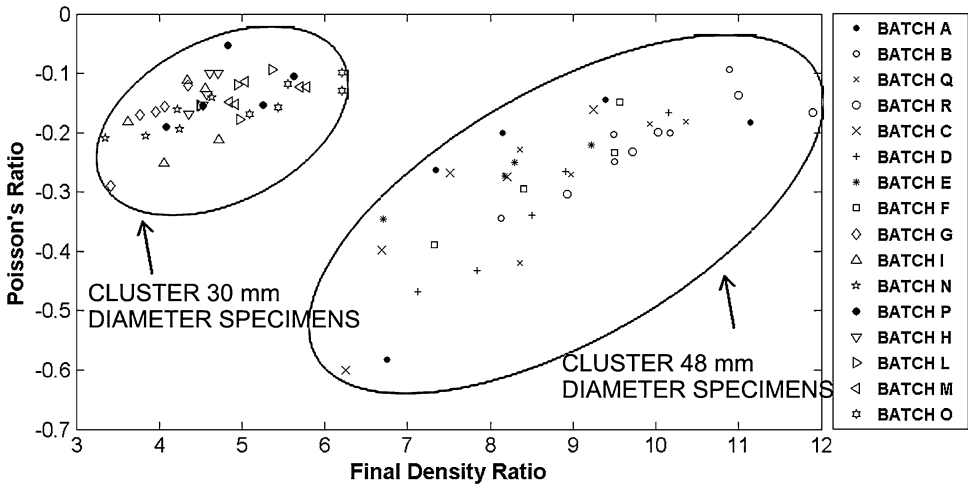

Fig. 6 Poisson's ratio versus final density ratio. The two clusters are shown bounded for clarity

obtained in batches A, C and D made from specimens of 48 mm of initial diameter and using the water-cooling method, with the maximal negative value in specimen 5C of −0.63. Specimen 5C had a processing temperature of 135 °C, and radial and axial compression ratios of 2.53 and 1.25, respectively. It appears that the batches can be divided into two main clusters, one containing specimens with an initial diameter of 30 mm (FDR ranging between 3.35 and 5.78 and v between −0.29 and −0.09), and the second containing specimens with an initial diameter of 48 mm (FDR values ranging between 6.25 and 11.90, and v between −0.63 and −0.10). All groups show a general monotonic dependence of the Poisson's ratio versus FDR values. The water-cooled batches with an initial diameter of 48 mm (A–D) have a higher value of correlation coefficient, with an average R^2 value of 0.80 and standard deviation of 20.6% of the mean correlation value. In contrast, batches with 30 mm initial diameter cooled in air at room temperature (M–P) are poorly correlated, with an average R^2 value of 0.49 and standard deviation of 39.2% of the mean correlation value. Almost certainly the water jet used to cool the mould provides a significant thermal shock and a more uniform temperature distribution during cooling, both in terms of exposure time and uniformity along the length of the mould, as opposed to air drying. Importantly no effect of the maximal temperature reached in the various batches that was observed.

In general, the largest magnitude negative Poisson's ratios were found for the specimens in each batch with the lowest FDR. The specimens 5A, 5C and 5G, with v values of −0.58, −0.63 and −0.59, respectively, showed the largest Poisson's ratios belonging to batches with final temperature of 135 °C and being water-cooled. It appears, however, that no specific correlation between cooling method and final temperature values exists in this case.

Figure 7 shows the behaviour of the tangent modulus versus the Poisson's ratio. Similar to Fig. 6, two clusters can be seen to emerge. While one cluster contains the specimens with an initial diameter of 30 mm, the less tightly packed cluster contains the batches with the

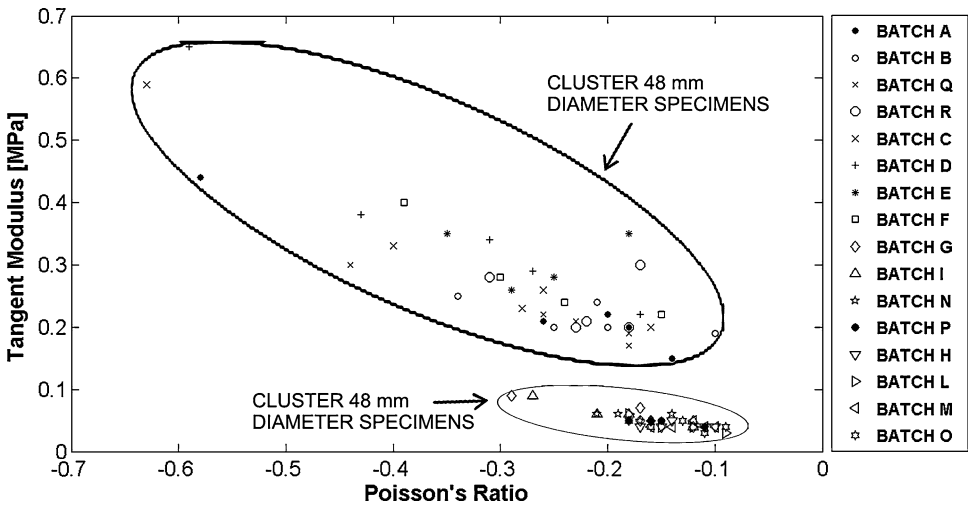

Fig. 7 Tangent modulus versus Poisson's ratio

specimens having 48 mm diameter. The first cluster shows a concentration of the specimens with stiffness between 0.03 and 0.09 MPa, while the second one is localised between 0.15 and 0.65 MPa. It is worth noting that the dependence of the tangent modulus versus the Poisson's ratio is in general monotonically decreasing, i.e., the modulus increases for large negative Poisson's ratio values.

A general decrease of the tangent modulus accompanied by the decrease of the Poisson's ratio was apparent, and a LLS best fit was derived for each batch. In general, the batches of specimens with initial diameters of 48 mm, with imposed length of 80 mm and water-cooled (i.e. C and D) showed a higher correlation with an average R^2 value of 0.94 and standard deviation 1% of the mean correlation value. Conversely, a condition of mean quasi-zero correlation occurred in several batches consisting of specimens with 30 mm initial diameter, room temperature-cooled. The water-cooled specimens 5A, 5C and 5D with initial diameter of 48 mm showed the higher values of stiffness (0.44, 0.59 and 0.65 MPa, respectively). Figure 8 shows the general monotonic stiffness (tangent modulus) versus the FDR decreases with the emerging of the two clusters. As with the previous analysis, the more concentrated cluster is related to batches made from specimens with 30 mm of initial diameter and the second to those with 48 mm of initial diameter.

Figure 9 shows how, in general, the energy dissipation decreases as Poisson's ratio approaches zero, albeit in this case there is no evident presence of clusters between batches made with specimens with 30 or 48 mm of initial diameter, nor is there a statistically significant correlation. It is worth noting that the 48 mm diameter specimens are more widely spread in comparison with specimens with the initial size of 30 mm.

Figure 10 shows the relation between stiffness and the tan δ between each stress–strain sinusoid. For this case, the modulus–loss grouping also shows the presence of the two clusters, as in Figs. 6–8.

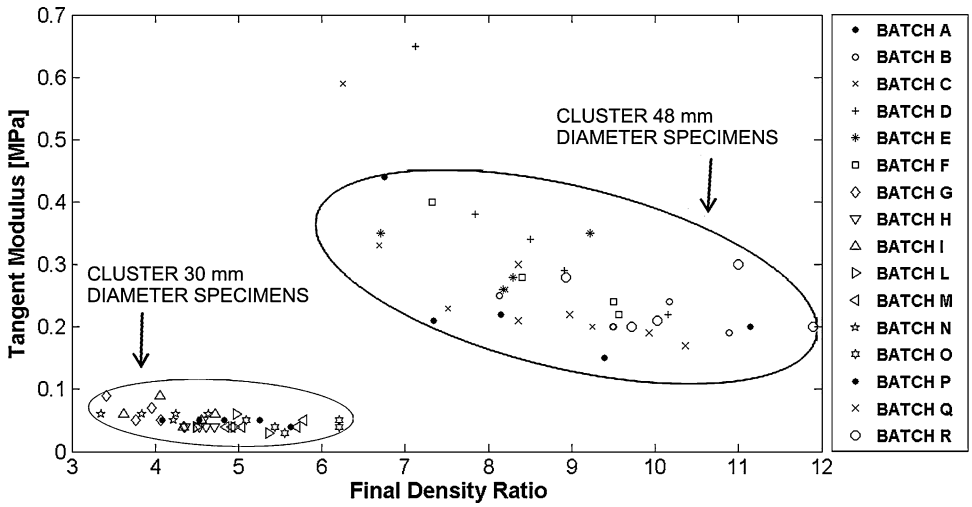

Fig. 8 Tangent modulus versus final density ratio

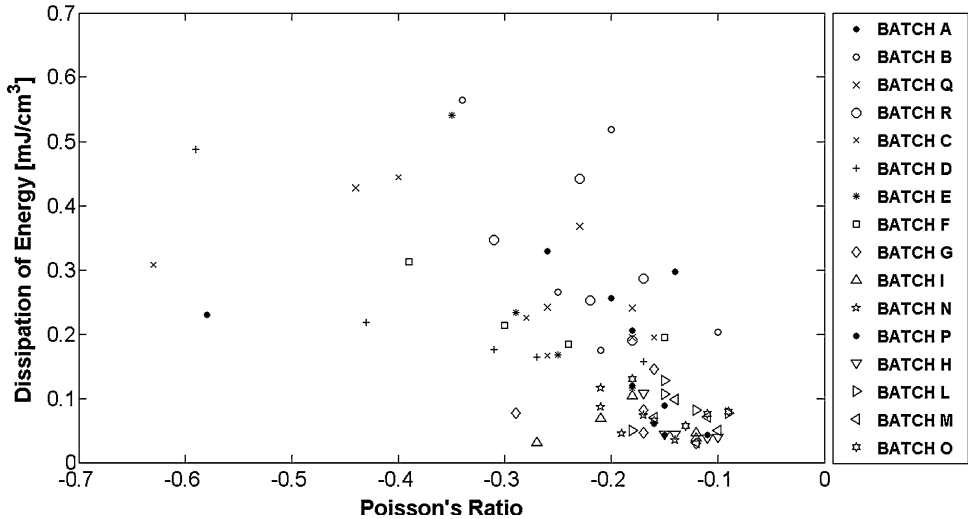

Fig. 9 Dissipation of energy versus Poisson's ratio

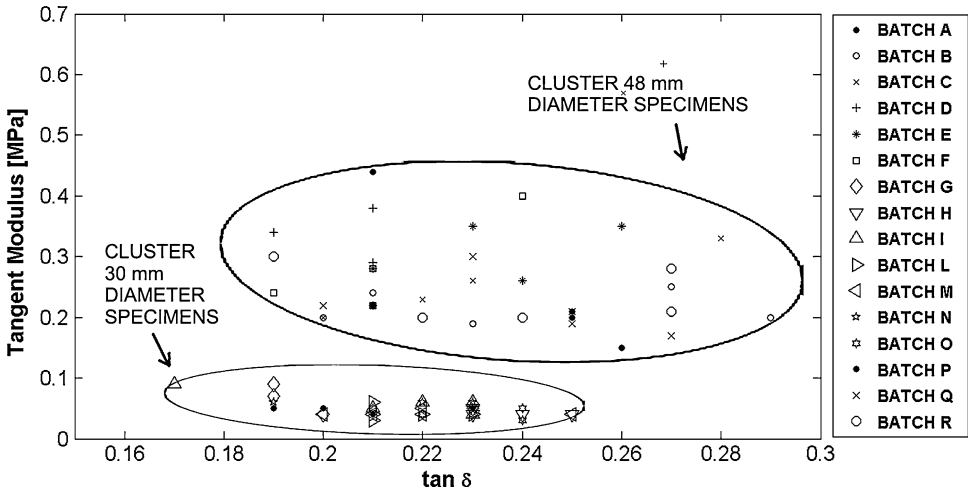

Fig. 10 Tangent modulus versus loss tangent

Five conventional foam specimens of 30 mm diameter were tested for reference. Their mean properties were as follows: $\nu = 0.62$, tangent modulus = 0.26 MPa, energy dissipation per unit volume = 0.92 mJ/cm^3, and tan $\delta = 0.33$. One specimen featured an outlier value of 0.401 mJ/cm^3 discarded using the Chauvenet's criterium [27]. The specific energy dissipation value is consistent with the ones recorded for conventional foams under compression–compression at small loading ratios [24].

The variation in processing parameters in this study is unique and so comparison with all the present specimens is not always possible simply because no other similar processed specimens exist. However, specimen 4C can be seen to match reasonably well data available from another study [22]. Specimen 4C has the largest magnitude negative Poisson's ratio in this study of −0.42, and a tangent modulus of 0.28 MPa. These values compare well with a Poisson's ratio of −0.22 and 'Young's modulus' (taken to be similar to tangent modulus in this study) of 0.21 MPa from [22]. The specimen from [22] was made from the same native foam and with similar initial dimensions to specimen 4C, but was converted to the auxetic state via a different compression, temperature profile and cooling method.

In broad terms the values of elastic properties presented here are within the range of those reported in the literature. One of the present authors has previously reported values for auxetic versions of another PU foams [19] of 0.02 MPa and 0.14 for tangent (given as Young's) modulus and loss factor, respectively. Another of the authors reported similar values of tangent modulus [28] of 17 kPa (0.017 MPa).

A study of the hysteresis loops on negative Poisson's ratio open cell foam has been carried out in [24], where the areas has been calculated from data gathered during fatigue tests performed at 3 Hz in compressive loading and under a preload of 70% of the initial length of each specimen. The results presented in this work provide lower values of energy dissipation (one order of magnitude on average); however one must consider that the testing conditions in [24] were very different (dynamic compressive preloaded versus quasi-static tensile without preload test). Reference [24] reports that the energy dissipation per unit volume of the native foam ($\sim$0.05 mJ/cm^3 after 20,000 cycles) is lower than the auxetic one (0.8 mJ/cm^3 as average result). The analysis carried out in the current work highlights a different behaviour. It is apparent in the results of the quasi-static cyclic tests that the conventional foam has a greater energy dissipation compared to the average value of the auxetic version (being 0.071 mJ/cm^3 for the auxetic specimens with an initial diameter of 30 mm). It is apparent that the overall compression is the most important factor in the determination of Poisson's ratio of these auxetic foams.

Conclusions

An established manufacturing process for producing thermoplastic auxetic cylinder foam from flexible PU foams specimens with an initial diameter of 30 and 48 mm has been modified, and the resulting auxetic foam mechanically tested. Density, Poisson's ratio, stiffness and dissipation of energy were identified for each specimen. Using the data acquired, a linear relation between FDR and imposed volumetric ratio for each auxetic specimen has been evaluated and a good value of correlation has been reached for each batch. All specimens were auxetic, with values of the Poisson's ratio ranging from −0.09 to −0.63. In each batch, the maximal negative Poisson's ratio was found in the specimens with the initial diameter of 48 mm, i.e. higher radial compression, but with the lowest FDR. In most cases, the stiffness of the specimens tested decreased for increasing FDR, and decreased with declining Poisson's ratio values. The water-cooled specimen with an

initial diameter of 48 mm showed the highest values of negative Poisson's ratio, while batches having an axial compression of 80 mm showed the best correlation between FDR and Poisson's ratio. Clusters of results found in the analysis made on the Poisson's ratio, FDR, stiffness and dissipation of energy suggest that the most important manufacturing factor is overall compression imposed. This is particularly evident in the relationship between tangent modulus and Poisson's ratio, where the 30 mm specimens tend to have lower modulus values than the 48 mm diameter samples. In contrast, no significant correlation between cooling methods, maximal temperature levels during the heating process and mechanical properties have been observed.

Acknowledgement The authors wish to express their gratitude to the anonymous reviewers for their useful comments.

References

1. Lakes RS (1987) Science 235:1038. doi:10.1126/science.235.4792.1038
2. Lakes RS (1987) Science 238:551. doi:10.1126/science.238.4826.551-a
3. Evans KE, Nkansah MA, Hutchinson IJ (1991) Nature 353:124. doi:10.1038/353124a0
4. Herakovich CT (1984) J Compos Mater 18(5):447. doi:10.1177/002199838401800504
5. Clarke JF, Duckett RA, Hine PJ, Hutchinson IJ, Ward IM (1994) Composites 25(9):863. doi:10.1016/0010-4361(94)90027-2
6. Evans KE, Donoghue JP, Alderson KL (2004) J Compos Mater 38(2):95. doi:10.1177/0021998304038645
7. Evans KE, Alderson KL (1992) J Mater Sci Lett 11(24):573. doi:10.1007/BF00736221
8. Alderson KL, Fitzgerald A, Evans KE (2000) J Mater Sci 35(16):1573. doi:10.1023/A:1004830103411
9. Abdel-Sayed FK, Jones R, Burgens IW (1979) Composites 10:279
10. Masters IG, Evans KE (1996) Compos Struct 35:403. doi:10.1016/S0263-8223(96)00054-2
11. Scarpa F, Panayiotou P, Tomlinson G (2000) J Strain Anal 35(5):383. doi:10.1243/0309324001514152
12. Prall D, Lakes R (1996) Int J Mech Sci 39(3):305. doi:10.1016/S0020-7403(96)00025-2
13. Scarpa F, Blain S, Lew T, Perrott D, Ruzzene M, Yates JR (2007) Compos A Appl Sci Manuf 38(2):280. doi:10.1016/j.compositesa.2006.04.007
14. Friis EA, Lakes RS, Park JB (1988) J Mater Sci 23:4406. doi:10.1007/BF00551939
15. Lakes RS, Elms K (1993) J Compos Mater 27:1193. doi:10.1177/002199839302701203
16. Chen CP, Lakes RS (1989) Cell Polym 8(5):343
17. Lakes RS (1992) Cell Polym 11:466
18. Howell B, Prendergast P, Hansen L (1994) Appl Acoust 43(2):141. doi:10.1016/0003-682X(94)90057-4
19. Scarpa F, Ciffo LG, Yates JR (2004) Smart Mater Struct 13(1):49. doi:10.1088/0964-1726/13/1/006
20. Chan N, Evans KE (1997) J Mater Sci 32(22):5945. doi:10.1023/A:1018606926094
21. Gaspar N, Smith CW, Miller EA, Seidler GT, Evans KE (2005) Phys Status Solidi B 242(3):550. doi:10.1002/pssb.200460375
22. Scarpa F, Pastorino P, Garelli A, Patsias S, Ruzzene M (2005) Phys Status Solidi B 242(3):681. doi:10.1002/pssb.200460386
23. Scarpa F, Yates JR, Ciffo LG (2002) Proc Inst Mech Eng C J Mech Sci 216(12):1153
24. Bezazi A, Scarpa F (2007) Int J Fatigue 29(7):922. doi:10.1016/j.ijfatigue.2006.07.015
25. Lakes RS (1998) Viscoelastic solids. CRC Press, Boca Raton, FL
26. Smith CW, Wootton RJ, Evans KE (1999) Exp Mech 39(4):356. doi:10.1007/BF02329817
27. Taylor JR (1997) An introduction to error analysis, 2nd edn. University Science Books, Sausolito, pp 166–168
28. Smith CW, Lehman F, Wootton RJ, Evans KE (1999) Cell Polym 18(2):79